



ELSEVIER

Available online at [www.sciencedirect.com](http://www.sciencedirect.com)

SCIENCE @ DIRECT®

Vacuum 80 (2005) 258–263

VACUUM

SURFACE ENGINEERING, SURFACE INSTRUMENTATION  
& VACUUM TECHNOLOGY

[www.elsevier.com/locate/vacuum](http://www.elsevier.com/locate/vacuum)

# Simple vacuum experiments for undergraduate student laboratories

J.M.F. dos Santos\*

*Physics Department, University of Coimbra, P-3004-516 Coimbra, Portugal*

---

## Abstract

An overview of typical simple experiments, intended for didactic laboratory vacuum classes for undergraduate students majoring in Physics, Physics Engineering and Material Sciences, is presented. For all the experiments, the students perform actual measurements of characteristics of different vacuum components or material properties and compare the obtained results with the values tabulated in the literature: pumping speed measurements, leak measurements, outgassing rate determinations and roughing line conductance estimation. The use of a He leak detector allows the measurement of helium permeability constants for different materials and, with an RGA, students are able to perform quantitative measurements of isotopic abundances for gases like argon and krypton.

© 2005 Elsevier Ltd. All rights reserved.

---

## 1. Introduction

Improvements in vacuum science and technology have triggered its application to wide areas of knowledge and it now plays an important role in many different industrial and research environments. The increasing use of elaborate and well-designed vacuum systems leads to the need for well-trained staff and engineers in this area. The education and training of researchers and technicians by actual practice in laboratories has importance and significance in a field like vacuum science and technology. This is of particular

importance for undergraduate university education, given the limited time available for teaching those curricula.

It is very important for students' education and training that direct quantitative measurements can be obtained during the experimental work, rather than just the simple operation of vacuum systems and qualitative analysis. Simple experiments, allowing students to perform direct measurements of the characteristics of different vacuum components and material properties, are thus important.

We will describe simple experiments intended for didactic laboratory vacuum classes of undergraduate courses, where actual measurements are performed and compared with the values tabulated in the literature. These experiments are

---

\*Tel.: +351 239 410667; fax: +351 239 829158.

E-mail address: [jmf@gian.fis.uc.pt](mailto:jmf@gian.fis.uc.pt).

intended for five to six times 4-h laboratory classes of an introductory vacuum course for undergraduate students majoring in Physics, Physics Engineering and Material Sciences. Small high-vacuum systems are used with a rough vacuum gauge at both the high-vacuum chamber and mechanical pump inlet. This allows the monitoring of the pressure in the vacuum chamber during the roughing procedure and after the high-vacuum valve is closed.

Helium leak detectors and residual gas analysers have become common in both research and industrial environments. They have changed from luxury equipment, requiring expert handling, to economic, reliable and powerful monitoring instruments, which are relatively easy to use. Therefore, it is important to include these systems in the experimental training of students. A simple experiment, using a He leak detector to measure the helium permeability of different materials, is presented. With a residual gas analyser (RGA), students are able to perform quantitative measurements of isotopic abundances for gases like argon and krypton.

## 2. High-vacuum system description

The vacuum systems we use are typical high-vacuum systems for teaching purposes. They include a small oil diffusion pump backed by a rotary pump and attached to an ISO test dome [1,2]. This chamber has several ports, which are necessary for gas inlet, vacuum gauges and connections to other equipment, e.g. an RGA. A combined Pirani/Penning controller is used, allowing continuous pressure monitoring in the high-vacuum chamber, in the  $10^5$ – $10^{-5}$  Pa range, and a rough vacuum reading at the rotary pump inlet.

The rough-vacuum pressure monitoring in the high-vacuum chamber enables the evaluation of gas throughput that enters the chamber volume [3], due to a real leak or to the outgassing of materials inside the chamber, through the pressure-rise rate. This way, there is no need to use the inverted pipette method or any other flowmeter device in pumping speed measurements of both rotary pump and high-vacuum pump [4,5], when

using the constant pressure method. Similarly, the outgassing rates of different materials placed inside the high-vacuum chamber are obtained in a straightforward way by the pressure rise, due to the gas load flowing into the chamber coming from the outgassing of those materials [6]. The roughing line conductance can be determined through the reading of both Pirani gauges in the chamber and at the forepump inlet.

## 3. Rough vacuum experiments

### 3.1. Pumping speed measurements using the constant volume method

The pumping speed,  $S$ , is measured at the high-vacuum chamber and at the rotary pump inlet as a function of pressure,  $p$ , using the constant volume method: the chamber is filled with air at atmospheric pressure, and the time,  $t$ , required to pump it down to a certain pressure is measured by both Pirani gauges. From the plot of  $\log_e[p(t)]$ , the effective pumping speed is calculated using

$$S = -V d(\log_e p)/dt, \quad (1)$$

where  $V$  is the volume being pumped. Fig. 1 depicts typical results obtained by students for the pressure variation as a function of time, during the roughing procedure, for the pressure reading in the chamber ( $p_1$ ) and at the rotary pump inlet ( $p_2$ ). For pressures above 10 mbar, the data can be fitted

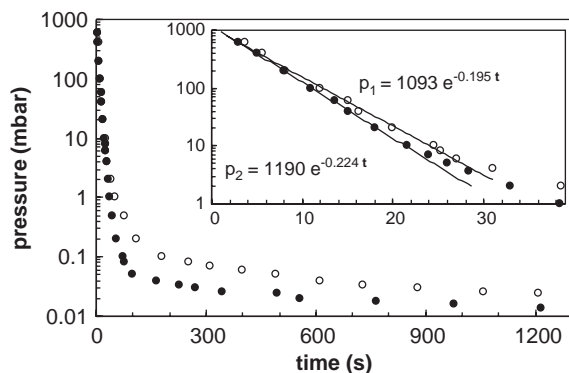


Fig. 1. Pressure evolution as a function of time in the high-vacuum chamber ( $p_1$ ) (○) and at the rotary pump inlet ( $p_2$ ) (●).

to a straight line with slope  $-(S/V)$ , i.e.  $S$  is independent of  $p$ . For lower pressures,  $S$  decreases due to the finite compression ratio of the pump and outgassing. The results obtained by different students for the pumping speed at the pump inlet are within 6% and agree with the manufacturer, while those obtained in the chamber are within 7%.

### 3.2. Pumping speed measurements using the constant pressure method

The forepump pumping speed is also determined by the constant pressure method: air is allowed to flow into the chamber through a needle valve and after equilibrium pressure  $p_{eq}$  is reached, the air throughput,  $Q$ , flowing into the chamber can be determined by valving off the pump and recording the pressure rise as a function of time.  $Q$  is then calculated using

$$Q = d(pV)/dt = Vdp/dt, \quad (2)$$

i.e. performing leak measurement by the pressure-rise rate method [7]. Fig. 2 depicts the pressure rise as a function of time for different  $p_{eq}$  in the chamber. The plot of  $p(t)$  is linear with slope  $Q/V$  since, for each opening position, the chamber volume is constant and the throughput of the gas flowing through the needle valve is also constant, illustrating the behaviour for a real leak. The

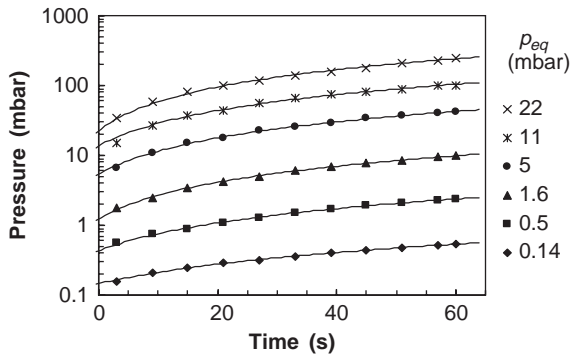


Fig. 2. Pressure evolution in the high-vacuum chamber as a function of time, after the rotary pump has been stopped, for different air leaks through the needle valve. The solid lines represent linear fittings to the different data sets.  $p_{eq}$  is the equilibrium pressure reached in the chamber while the pumping action was on.

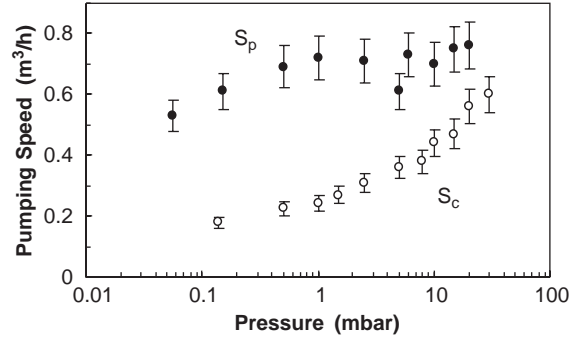


Fig. 3. Rotary pump pumping speed as a function of pressure at pump inlet ( $S_p$ ) and in the high-vacuum chamber ( $S_c$ ).

difference between real and virtual leaks is established: for a virtual leak (needle valve closed) the pressure in the chamber rises towards an equilibrium pressure.

The pump speed is obtained through

$$S = Q/(p_{eq} - p_u), \quad (3)$$

where  $p_u$  is the ultimate pressure achieved in the high-vacuum chamber. These values can be compared with those obtained with the constant pressure method, and present more accurate results at lower pressures (see Fig. 3).

### 3.3. Leak valve calibration and roughing line conductance determination

The measurement of  $Q$  for each opening position of the needle valve,  $NV_{pos}$ , allows the valve calibration curve,  $Q(NV_{pos})$ , to be obtained. On the other hand, the roughing line conductance,  $C$ , may be calculated through

$$C = Q/(p_{eq1} - p_{eq2}), \quad (4)$$

where  $p_{eq1}$  and  $p_{eq2}$  are the equilibrium pressure readings of the Pirani gauges placed in the chamber and at the forepump inlet, respectively, for each needle valve opening position. It is, thus, possible to obtain a plot of  $C$  as a function of the average pressure ( $p_{av}$ ) between  $p_{eq1}$  and  $p_{eq2}$ .

Fig. 4 depicts a typical behaviour for  $C(p_{av})$ . The approximately linear dependence of  $C$  results from the fact that the air flow through the roughing line is predominantly in the laminar regime for the pressures studied. Fig. 3 depicts the

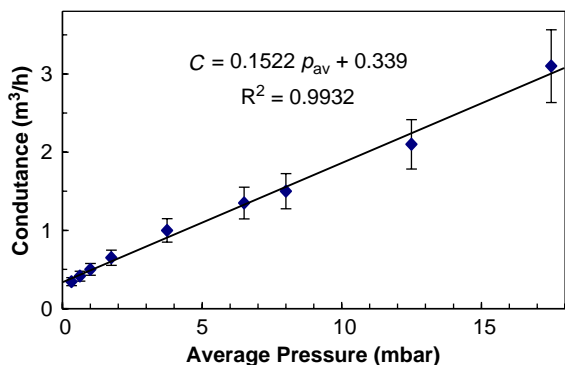


Fig. 4. Roughing line conductance as a function of average pressure at the ends of the line. The solid line represents a linear fitting to the data.

rotary pumping speed in the chamber and at the rotary pump inlet as a function of pressure, using  $p_{eq1}$  and  $p_{eq2}$ , respectively, in Eq. (3). While the effective pumping speed at the pump inlet is fairly constant, decreasing slowly for pressures below 0.5 mbar, the pumping speed in the chamber experiences a significant reduction for pressures lower than about 10 mbar, due to decrease of the roughing line conductance.

## 4. High-vacuum experiments

### 4.1. Pumping speed measurements

The high-vacuum pump speed can be determined by the constant pressure method, as was done for the forepump in Section 3.2. After the equilibrium pressure has been reached in the chamber (in the  $10^{-2}$ – $10^{-5}$  Pa range), the high-vacuum valve is closed and the pressure rise in the chamber as a function of time is monitored in the Pirani gauge. The pressure rise method can be used for throughput determinations [4,5] instead of a flowmeter. The results obtained for  $Q(NV_{pos})$  will complement those obtained in Section 3.3. The pumping speed measurements obtained by the different students normally agree within 10%. It should be pointed out to the students that the calculated values obtained for the pumping speed depend on the accuracy and precision of the absolute measurement of  $p_{eq}$  in the Penning gauge,

which should be calibrated in a qualified laboratory for such measurements.

### 4.2. Outgassing rate measurements

The gas throughput due to the outgassing of test samples placed in the high-vacuum chamber can be estimated by the pressure rise after the high-vacuum valve has been closed [6]. This outgassing can be taken as a virtual leak and, after the high-vacuum valve has been closed, the pressure in the chamber will rise towards an equilibrium. However, for pressures much lower than this equilibrium, a nearly linear rise is observed, and the gas throughput due to outgassing can be estimated.

Background outgassing is the main limiting factor and can be estimated by the pressure-rise rate obtained for the empty sample chamber. To reduce its contribution, the high-vacuum chamber can be baked and we have used an independent small sample chamber, connected to the high-vacuum chamber through an isolation valve. In this way, only the surfaces of the small chamber are exposed to the atmosphere during sample handling.

Typical pressure rise as a function of time is depicted in Fig. 5 for background, Vor, Viton and Teflon samples. In each case, the samples were pumped for half an hour. The outgassing throughput is obtained using Eq. (2) and the sample

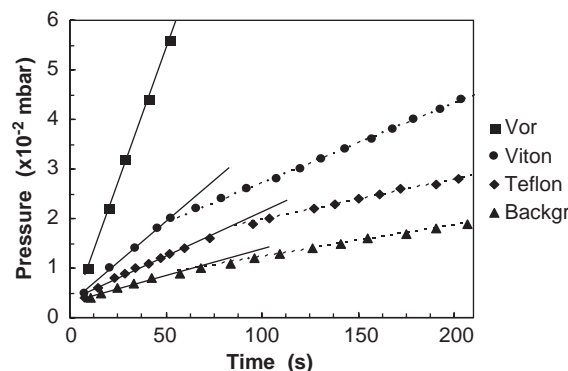


Fig. 5. Pressure rise in the high-vacuum chamber as a function of time, after the high-vacuum valve has been closed, for the different samples present inside the sample chamber. The solid and broken lines present linear fittings to the different data points in the lower and higher pressure regions, respectively.

outgassing rate ( $q_{1/2}$ ) is obtained through

$$q_{1/2} = (Q - Q_0)/A, \quad (5)$$

where  $Q_0$  is the background outgassing throughput and  $A$  is the surface area of the sample. For the example presented in Fig. 5, the results obtained for Viton and Teflon outgassing rates are 30% lower when the second slope of the curves, at higher pressures, is used instead of the first slope. As an example, for Vor, the results obtained by the different students extended through almost a decade, with a relative standard deviation of about 60%. Nevertheless, the obtained results are in reasonable agreement with those reported in the literature [8].

## 5. Experiments using a helium leak detector

An experiment can be designed not only to acquaint the student with the use of the helium leak detector, finding a leak in a vacuum component and measuring its leak rate, but it may also be used to measure the permeability of materials. Actually, the gas throughput,  $Q$ , flowing into the chamber volume due to material permeability, can be taken as a real leak, obeying approximately the general expression

$$Q = K(A/d)\Delta p, \quad (6)$$

where  $A$  is the area of the material for which the permeability is being measured,  $d$  is its thickness and  $\Delta p$  is the differential pressure between the two sides of the material. Students can assess the dependence of  $Q$  on  $A$ ,  $d$  and  $\Delta p$ , for different materials such as plastic foils and quartz thin discs.

The experimental setup may be a simple flange to which the material under study is glued with epoxy, separating two volumes: one connected to the leak-detector port and the other to the helium admittance line. A blank flange with a stainless-steel disc glued with epoxy to it can be used to determine the background flow due to helium permeability through the epoxy.

In Fig. 6 we depict experimental results of the leak rate through 1-cm-diameter Kapton foils as a function of thickness, for 1 bar helium pressure differential. The helium leak-detector was

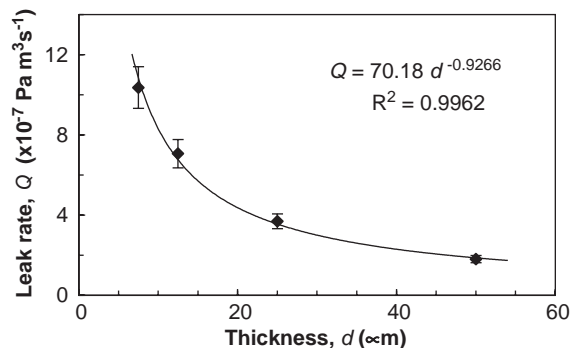


Fig. 6. Helium leak rate due to permeability through 1-cm-diameter Kapton foils as a function of their thickness for 1 bar helium pressure differential. The solid line is the best fit to the experimental data.

equipped with a calibrated leak allowing absolute  $Q$  measurements. The results obtained for the Kapton permeability constant are in good agreement with those reported in the literature [9].

## 6. Experiments using an RGA

Students can become acquainted with several simple uses of an RGA: determination of qualitative air composition, residual gas analysis in the diffusion pump system and cracking patterns. Nevertheless, changes in the operating conditions and history of a given RGA affect its sensitivity and the obtained cracking pattern spectrum of a given gas [9,10]. Thus, the patterns given in tables are intended to be representative and are not unique, although there are enough similarities justifying their tabulation. This is a drawback for quantitative measurement and comparison of the results with the literature.

The measurement of natural abundances of the different isotopes of a given element is a simple straightforward experiment to be performed with a RGA, and the results can be compared with those tabulated in the literature. Given the small mass range of the different isotopes and the same species of atoms and/or molecules of the sample gas, the sensitivity of the residual gas analyser is fairly constant for all isotopes. Additionally, as the isotope abundance is given by the respective peak

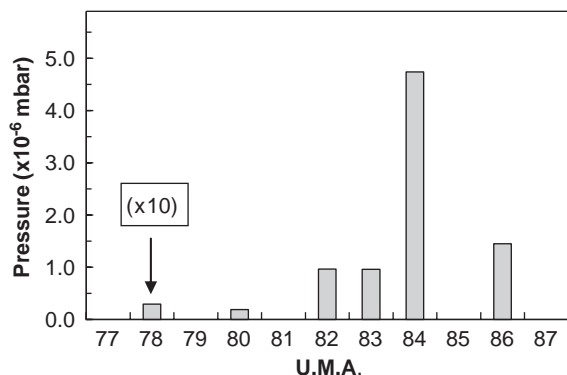


Fig. 7. Typical RGA partial pressure measurement in the mass range of 77–87 amu for a krypton leak introduced in the vacuum chamber.

height relative to the total sum of the different peak heights corresponding to all isotopes, the obtained experimental results are independent of the mass spectrometer operating conditions and agree well with the tabulated results (e.g. [11]). Fig. 7 depicts a typical scan, obtained by the RGA, of the partial pressures for the mass range of 77–87 amu, for a krypton leak introduced in the vacuum chamber.

## 7. Conclusion

We have prepared a set of basic experiments covering a wide range of theoretical and practical

techniques underlying vacuum technology, and fitting in the limited time available for vacuum science and technology laboratory classes for university undergraduate students. Common to all the experiments is the fact that, during the course of the experimental activities, actual measurements of characteristics of different vacuum components or material properties are performed and compared with the values tabulated in the literature.

## References

- [1] Draft International Standard. ISO/R—1608(1). 1970.
- [2] Sharma JKN, Sharma DR. *Vacuum* 1982;32(5):253.
- [3] dos Santos JMF. *Eur J Phys* 1990;11:130.
- [4] dos Santos JMF. *Vacuum* 1988;38(7):541.
- [5] Muhlenhaupt RC. *J Vac Sci Technol* 1982;20(4):1005.
- [6] dos Santos JMF, Bento ACSSM, Reyes Cortes SD, Dias THVT. *Eur J Phys* 1990;11:249.
- [7] American Vacuum Society 1968. Standard AVS 2.2-1968. *J Vac Sci Technol* 1968;5(6):219.
- [8] Henry RP. *Le Vide* 1969;144:316.
- [9] Weston GF. *Ultrahigh vacuum practice*. London: Butterworths; 1985. p. 55.
- [10] O'Hanlon JF. *A Users Guide to Vacuum Technology*, 3rd ed. New York: Wiley; 2003.
- [11] dos Santos JMF, Trindade AMF, Veloso JFCA, Monteiro CMB. *Eur J Phys* 2004;25:469.